AeroSense'96
Algorithms for Multispectral and Hyperspectral Imagery
Conference 2758

Los Alamos National Laboratory

ACCURATE TOP OF THE ATMOSPHERE ALBEDO DETERMINATION FROM MULTIPLE VIEWS OF THE MISR INSTRUMENT

Christoph C. Borel, Siegfried A. W. Gerstl
MS C323, Los Alamos National Laboratory, Los Alamos, NM 87545, USA
Carmen Tornow
German Aerospace Research Establishment, Rudower Chaussee, 12484 Berlin

1. Introduction

   Definition of TOA Albedo

2. Simulated MISR Data Set: JMRT Code
3. Azimuthal Models for the Top of the Atmosphere Reflectance: AZM, CSAR, Uniqueness, Noise Sensitivity
4. Clear Sky Top of Atmosphere Albedo Algorithm
5. Results: 4 Models
6. Conclusions

Introduction

Multi-angle Imaging Spectro-Radiometer (MISR):

- EOS-AM platform, launch in 1998
- Nine cameras - zenith angles of ±70.5, ±60, ±45, ±26.1 and 0 degrees in the along track direction
- Four spectral channels: 443 nm (blue), 550 nm (green), 670 nm (red) and 865 nm (near infrared)
- Misc: 275m pixels, 360 km swath, 9 day repeat
- Global Data Products: (georeferenced)
  - Top of the atmosphere spectral albedo (2.1km and 31km) (clear and cloudy conditions)
  - Surface hemispherical-directional reflectance factor (ocean: 2.1km and land: 1.1km),
  - Aerosol distributions (ocean: 2.2km and land: 17.6km).

Definition of TOA Albedo

The albedo in each MISR channel c, $c = [1, 2, 3, 4]$ is defined according to Nicodemus et al, 1977, as:

$$\alpha_{0,c}(\mu_s) \;=\; \frac{1}{\pi} \int_0^1 d\mu_v \mu_v \, \int_0^{2\pi} d\phi_v \; BRF_c(\mu_s, \mu_v, \phi_v), \tag{1}$$

with the notation:

$\alpha_{0,c}(\mu_s)$ is the top of atmosphere albedo in MISR channel c,

ϕ_v is the angle relative to the solar azimuth,

μ_s is the cosine of the solar zenith angle θ_0,

μ_v is the cosine of the view zenith angle θ and

$BRF_c(\mu_s,\, \mu_v,\, \phi_v)$ is the bidirectional reflectance factor in MISR channel c.

Relationship between the BRF and the bidirectional reflectance distribution function $BRDF$ is:

$$BRDF_c(\mu_s, \mu_v, \phi_v) \; = \; \frac{1}{\pi} BRF_c(\mu_s, \mu_v, \phi_v). \tag{2}$$

The BRF_c is related to the radiance L_c by the following equation:

$$BRF_c(\mu_s, \mu_v, \phi_v) \; = \; \frac{\pi \; L_c(\mu_s, \mu_v, \phi_v) \; D^2}{\mu_s \; E_{0,c}}, \tag{3}$$

where $D = R(t)/R_0$ is the normalized distance to the sun. $R(t)$ is the time dependent distance and R_0 is the distance for which E_0 is defined and E_0 is the TOA solar irradiance.

Simulated MISR Data Set

Motivation:

- No MISR data yet available
- Clear sky TOA albedo algorithm must be available at launch

Requirements for simulated data set:

- "Radiative transfer" (RT) code must include BRDF
- Must calculate the multiple scattering for a large range of sun and view angles
- Radiance with an error less than 1% requires an eight stream approximation (two stream approximations can cause up to 20% error)

Two available codes: 6S (Vermote et al, 1994) and JMRT (Martonchik, 1994).
(MODTRAN3 was not was not available prior to this work)

"John Martonchik Radiative Transfer" (JMRT) Code

Features:

- Five different aerosol types (urban, rural, maritime, desert and arctic)
- 46 surface BRDF's from experimental data and models:
  - vegetation (23),
  - bare soil (3),
  - rough water surface (11),
  - snow and ice (9).
- Computes BRF in 10 zenith and 12 azimuthal angles
- Any additional surface BRDF's can be added
- Number of streams is variable

Albedo calculation:

- Simulated MISR data set uses 1-step Newton-Cotes integration:

$$\alpha_{0,c}(\mu_s) \;=\; Const\frac{2\pi}{N_\phi - 1}\sum_{i=1}^{N_\theta - 1}\;\mu_l\;\sum_{j=1}^{N_\phi - 1}\frac{\mu_i BRF_c(\mu_i,\phi_j) + \mu_{i+1}BRF_c(\mu_{i+1},\phi_j)}{2(\mu_{i+1}-\mu_i)}, \qquad (4)$$

  where $N_\phi = 12$ is the number of azimuthal and $N_\theta = 10$ is the number of elevation angles, $Const$ is determined by setting $\alpha_0(\mu_s) = 1$ with $BRF_c(\mu_v,\phi_v) = 1$ in eq.(4).

- Inverted BRF model uses numerical integration with iterated Gaussian quadrature over μ_v and ϕ_v

Azimuthal Models for the TOA BRF

Purpose and Requirements :

- MISR measures only in nine discrete directions ⇒ estimate the TOA radiance in directions which are not seen by MISR
- Azimuthal model (AZM) described BRF in other directions ⇒ semi-empirical function
  - As few parameters as possible,
  - Uniquely invertible
  - Reciprocal (sun and view angles are interchangeable without changing the value)
  - Little sensitivity to noise.

Coupled Surface-Atmosphere Reflectance (CSAR)

$$BRF_{CSAR}(\theta_s, \phi_s; \theta_v, \phi_v) \;=\; \varrho_0 \frac{\mu_s^{\kappa-1} \mu_v^{\kappa-1}}{(\mu_s + \mu_v)^{1-\kappa}} F(g)[1 + R(G)], \tag{5}$$

where ϱ_0 and κ are empirical surface parameters between 0 and 1 with the condition on ϱ_0 that the albedo of eq.(5) is between 0 and 1, and $F(g)$ is the Henyey-Greenstein function:

$$F(g) = \frac{1 - \Theta_0^2}{[1 + \Theta_0^2 - 2\Theta_0 \cos(\pi - g)]^{1.5}}$$

Θ_0 controls the forward ($0 \leq \Theta_0 \leq 1$) and backward (hot spot) ($-1 \leq \Theta_0 \leq 0$) scattering peak, g is a phase angle and given by: $\cos g = \mu_s \mu_v + \sin\theta_s \sin\theta_v \cos(\phi_s - \phi_v)$, $(1 + R(G))$ approximates the hot-spot with:

$$1 + R(G) = 1 + \frac{1 - \varrho_0}{1 + G},$$

where $G = \sqrt{\tan^2\theta_s + \tan^2\theta_v - 2\tan\theta_s \tan\theta_v \cos(\phi_s - \phi_v)}$.

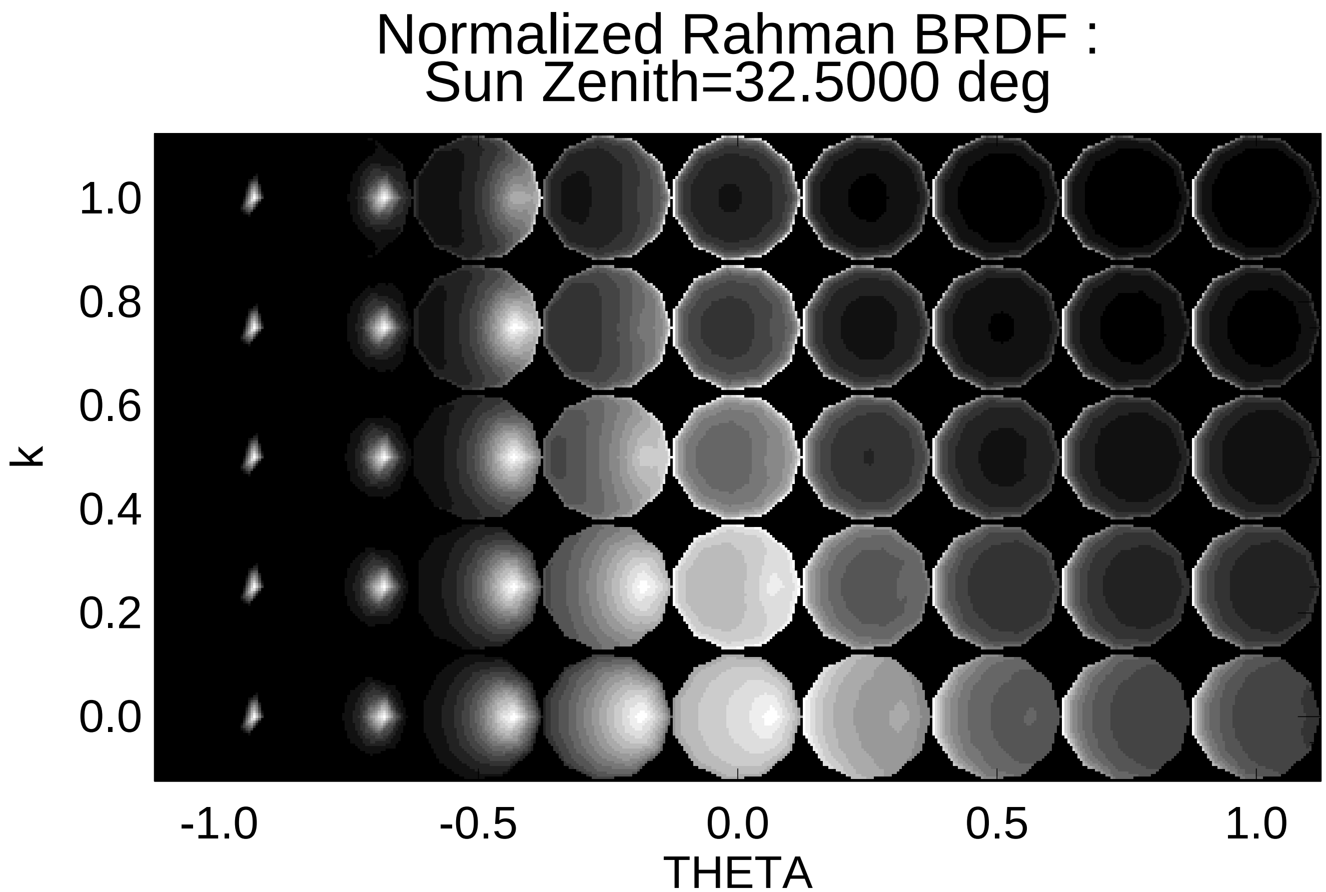

Polar representation of the CSAR BRF for $\theta_s = 32.5^o$ and $\varrho_0 = 0.2$ as a function of Θ_0 and κ.

Uniqueness

Problem:

Given a BRF slice for a given CSAR parameter set ($\varrho_0,\ \kappa$ and Θ_0) can we recover the original parameter set using non-linear least square fitting?

Procedure:

1. Generate N_p randomly chosen parameters: $\varrho_{0,i},\ \kappa$ and $\Theta_{0,i},\ i = 1, 2, 3, \ldots, N_p$.
2. Calculate N_p BRF slices $BRF(\theta_s, \phi_s; \vec{\theta_v}, \vec{\phi_v}; \varrho_{0,i},\ \kappa,\ \Theta_{0,i})$ using eq.(5).
3. Invert BRF model for $\widehat{\varrho_{0,i}},\ \hat{\kappa}$ and $\widehat{\Theta_{0,i}}$.
4. Compute errors $\varepsilon(\varrho_{0,i}) = \widehat{\varrho_{0,i}} - \varrho_{0,i}$, $\varepsilon(\kappa) = \hat{\kappa} - \kappa$ and $\varepsilon(\Theta_{0,i}) = \widehat{\Theta_{0,i}} - \Theta_{0,i}$ and the "Root Mean Square Error" (RMSE) of the BRF slice difference $(B\widehat{RF}_i - BRF_i)$.

Result: Yes, the CSAR model appears unique

Noise Sensitivity

Problems:

(A) How much noise can be tolerated in the inversion? (B) How does the albedo error change as a function of added noise?

Procedure:

1. Generate a BRF slice BRF for a fixed set of parameters: $\theta_s = 30^o$, $\varrho_0 = 0.5$, $\kappa = 0.3$ and $\Theta_0 = 0.22$ and compute the albedo α_0 using a numerical integration technique (e.g. 1-step or 5-step Newton-Cotes integration).
2. For $i = 1, \ldots, N_p$ cases do:
   (a) $BRF_i = BRF + \sigma_i N_i(0,1)$, where $N(0,\sigma_i)$ denotes the i-th realization of a Gaussian distributed random vector with mean 0 and standard deviation σ_i where $\sigma_i = \{1,2,3,\ldots,N_p\}\Delta_\sigma$ and Δ_σ is an increment.
   (b) Retrieve the BRF parameters: $\widehat{\varrho_{0,i}}$, $\hat{\kappa}$ and $\widehat{\Theta_{0,i}}$ and the fitted $B\widehat{R}F_i$. Compute the albedo $\widehat{\alpha_0}$ of the inverted BRF.
3. Plot the BRF, BRF_i and $B\widehat{R}F_i$ as a function of MISR camera angle.
4. Plot σ_i on the x-axis and $[(\alpha_0 - \widehat{\alpha_{0,i}}), (BRF - B\widehat{R}F_i), (\varrho_0 - \widehat{\varrho_{0,i}}), (\kappa - \hat{\kappa}), (\Theta_0 - \widehat{\Theta_{0,i}})]$ on the y-axis.

Results: (A) The error between original and retrieved BRF parameters grows linearly with increased noise. (B) The albedo error was less than $\pm 5\%$ for $\sigma \leq 0.1$ for an albedo of 0.43.

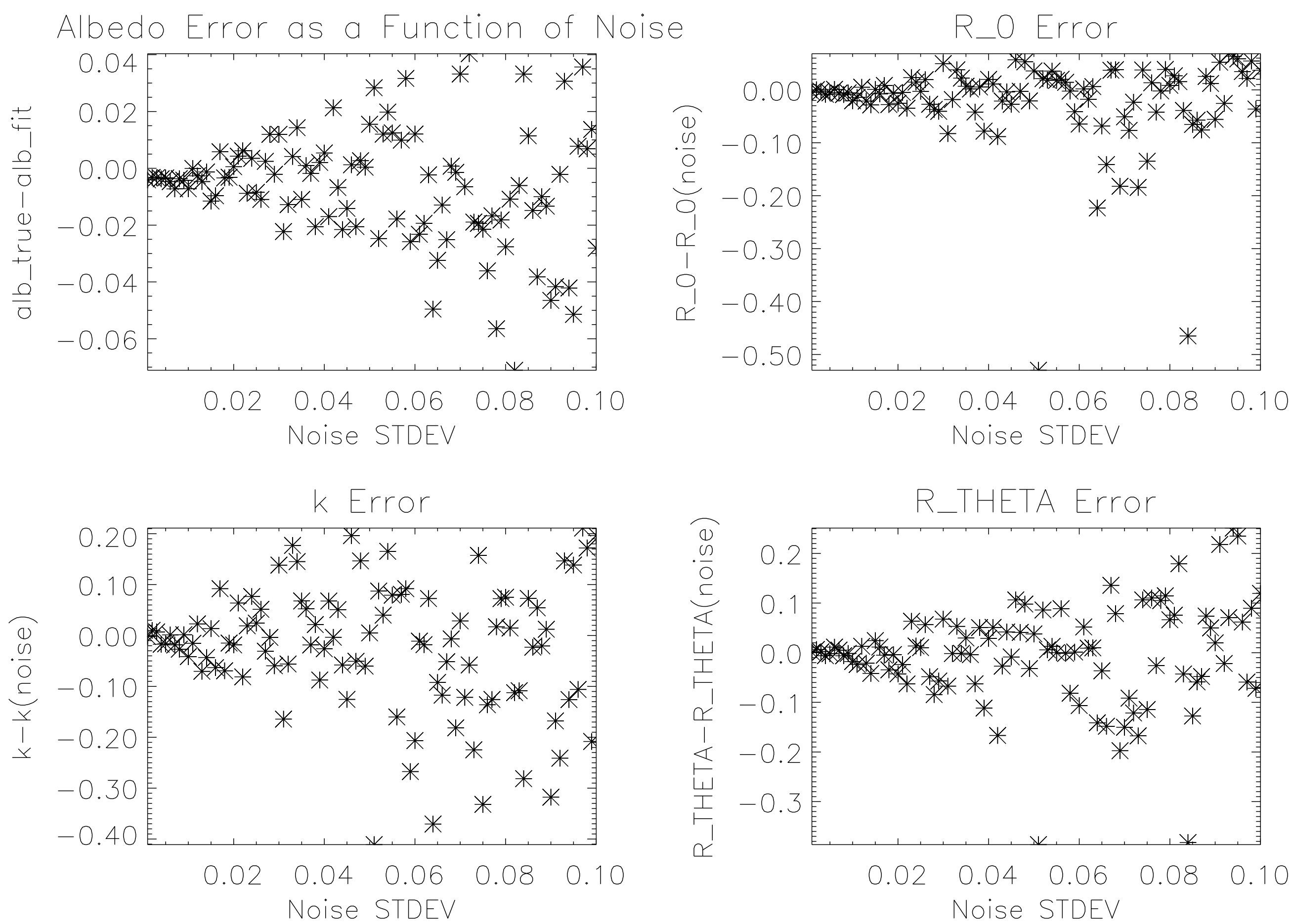

Clear Sky Top of Atmosphere Albedo Algorithm

1. Read TOA BRFs from JMRT output.
2. For all N_k cases $k = 1, 2, 3, \ldots, N_k$ do:
   (a) Compute the albedo $\alpha_{0,k}$ using Newton-Cotes integration over the quadrature angles.
   (b) For view azimuthal angles $\phi_j = [0^o,\ 30^o,\ 60^o,\ 90^o]$ do:
      i. Extract a BRF slice $(BRF_i,\ i = 1, 2, \ldots, 9$ at the MISR angles for $(\phi_j,\ \phi_j + 180^o)$.
      ii. Perform nonlinear curve fit of $BRF_{j,i}$ results in estimated CSAR parameters $\widehat{\varrho_{0,j,k}},\ \widehat{\kappa_{j,k}}$ and $\widehat{\Theta_{0,j,k}}$.
      iii. Do a numerical integration of CSAR model over the hemisphere results in estimated albedo $\widehat{\alpha_{0,j,k}}$.
      iv. Compute albedo error $\varepsilon(\alpha_{0,j,k}) = \alpha_{0,k} - \widehat{\alpha_{0,j,k}}$.
   (c) Plot standard deviation σ of the albedo error $\varepsilon(\alpha_{0,j,k}(\phi_j))$
   (d) Generate TOA BRF from estimated CSAR parameters and display.
3. Generate scatter plots of standard deviation of the albedo error versus azimuth marking different surface types with symbols.

Results

Error Metric:

Standard deviation σ of the albedo error

Cases:

- 5 different atmospheres
- 3 sun angles $(15^o,\ 32.5^o,\ 50^o)$
- 4 different azimuthal angles at $(0^o,\ 30^o,\ 60^o$ and $90^o)$

$\Rightarrow$ 2760 cases
Computing time: $\approx$ 1h on Sparc 10 (includes visualization)
Note: Faster inversion routines must be found to make this approach practicable for the EOS data information system

Three Parameters (no Limits) CSAR Model

Motivation: Easy to perform nonlinear least squares curve fit without bounded parameters

$$BRF_1(\theta_i, \phi_i) = BRF_{CSAR}(\theta_i, \phi_i; \varrho_0, \kappa, \Theta_0), i = 1, \ldots, 9 \tag{6}$$

Result: For snow and ice which have larger reflectances and a more Lambertian character, the errors exceeded the 5% level for many azimuthal angles.

Reason: The inversion routine which was not able to find a good solution in the 20 iteration limit and RMSE error limits of 0.001.

Three Parameters (no Limits) CSAR Model

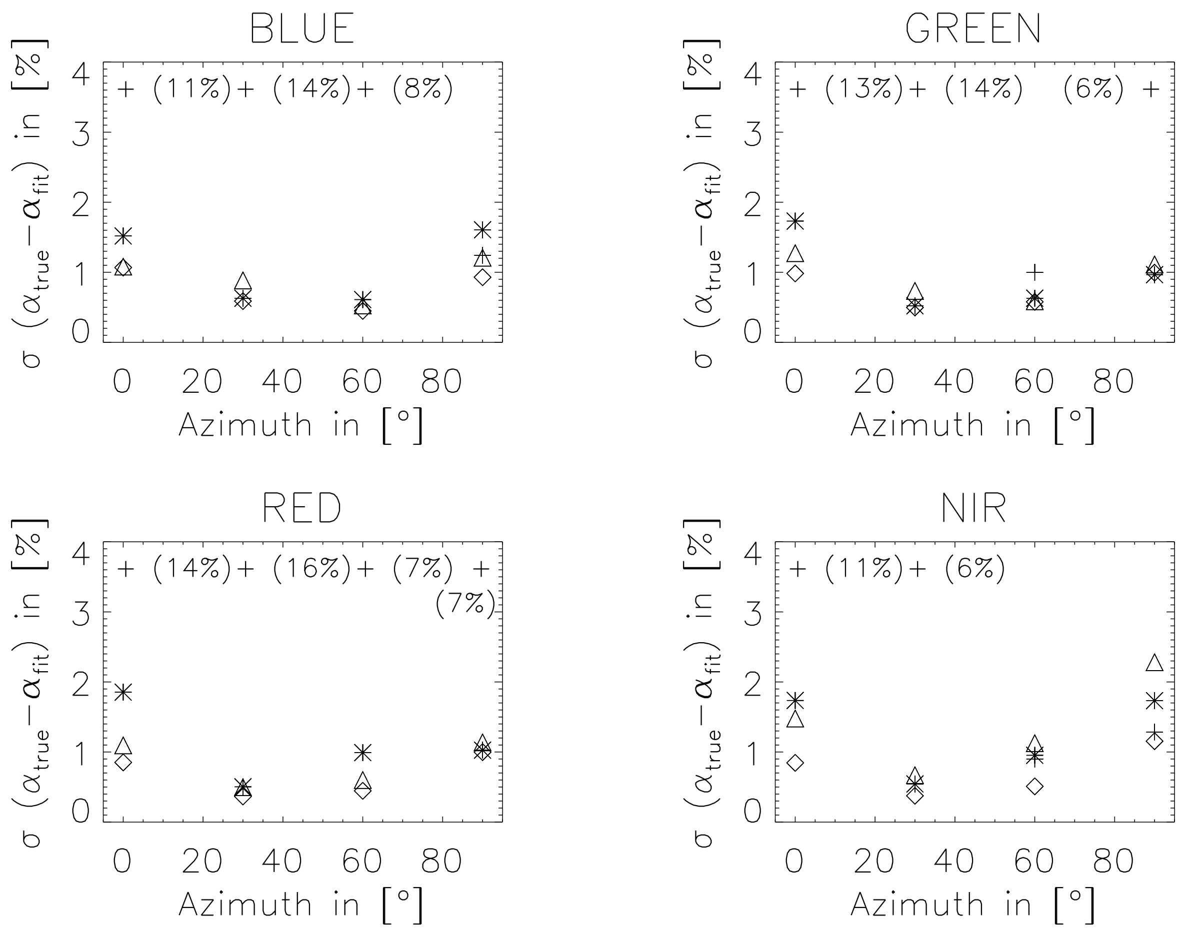

Symbols used: △ Vegetation (23 models), ◇ Soil and sand (3 models), + Snow and ice (9 models) and $*$ Water (11 models). Note: plot data points outside the 4% limit as symbols with an error in % in brackets.

Two Parameters (with Limits) CSAR Model

Motivation: MISR does not measure in the principle plane $\Rightarrow$ do not use parameter which models forward or backward scattering

$$BRF_2(\theta_i, \phi_i) = BRF_{CSAR}(\theta_i, \phi_i; \varrho_0', \kappa', F(g) = 1), \quad i = 1, \ldots, 9. \tag{7}$$

Variable transform: from the original unbound variable ϱ_0 to the interval limited variable ϱ_0' was used:

$$\varrho_0' = \frac{1}{2} + \frac{\tan^{-1}(\varrho_0)}{\pi}$$

and it's inverse:

$$\varrho_0 = \tan(\pi(\varrho_0 - \frac{1}{2})).$$

Similarilly κ can be transformed to κ'.

Result: The method works well for all cases and channels ($\sigma < 3.8\%$) For more typical MISR azimuthal angles between 30^o and 60^o the albedo errors are below 2% which is very good.

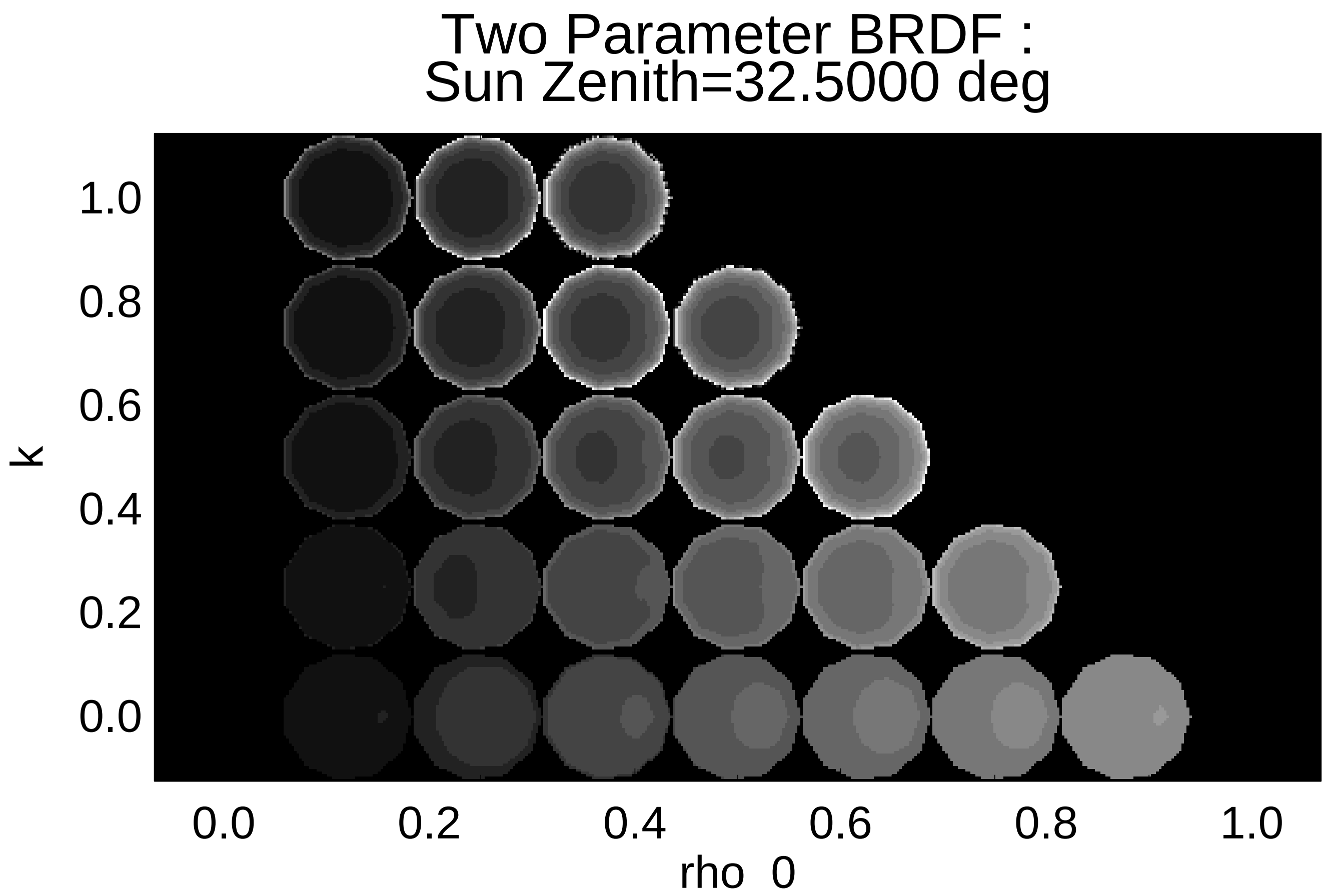

Polar representation of the two parameter CSAR BRF for $\theta_s = 32.5^o$ as a function of ϱ_0 and κ.

Two Parameters (with Limits) CSAR Model

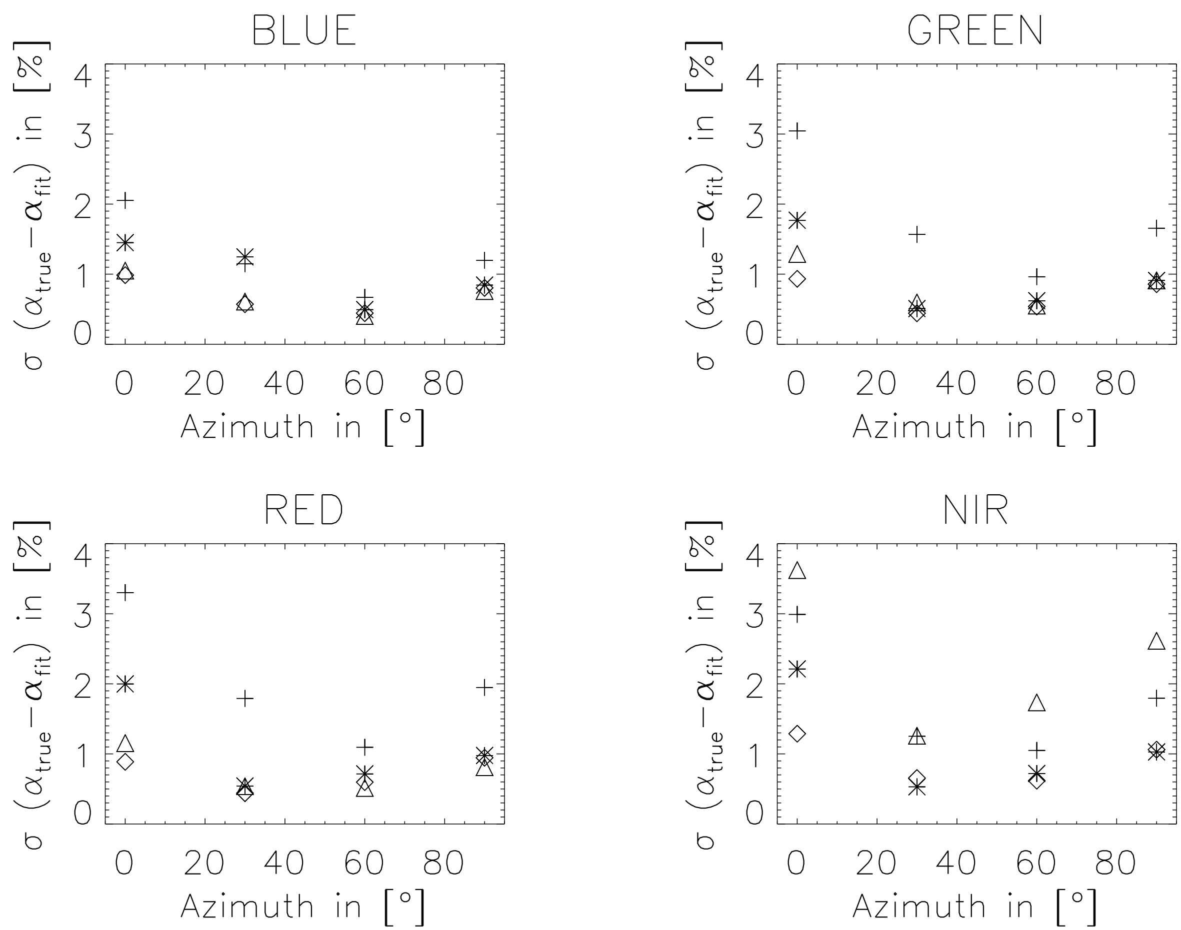

Symbols used: △ Vegetation (23 models), ◇ Soil and sand (3 models), + Snow and ice (9 models) and $*$ Water (11 models).

Atmospheric Transmission Correction

Motivation: Visualizing the resulting TOA BRF fields for the BRF_1 and BRF_2 models we noticed that the BRF near the horizon $(80^o < \theta_v < 90^o)$ often was very much larger than the computed BRF from JMRT.

Idea: Include atmospheric terms, e.g. transmission.

$$BRF_3(\theta_i, \phi_i) = BRF_{CSAR}(\theta_i, \phi_i; \varrho_0, \kappa, \Theta) \exp(-\tau_c/\mu_i), \quad i = 1, \ldots, 9; \; c = 1, 2, 3, 4 \qquad (8)$$

where the mean transmission factor $T_c = \exp(-\tau_c/\mu_i)$ and $\tau_c = [.24, .094, .043, .015]$ and c is the channel indicator.

Result: Works well for blue channel and in the principle plane $\phi = 0^o$. Converges for all cases for the NIR to less than 3.8% σ.

AeroSense'96
Algorithms for Multispectral and Hyperspectral Imagery
Conference 2758

Los Alamos National Laboratory

Atmospheric Transmission Correction

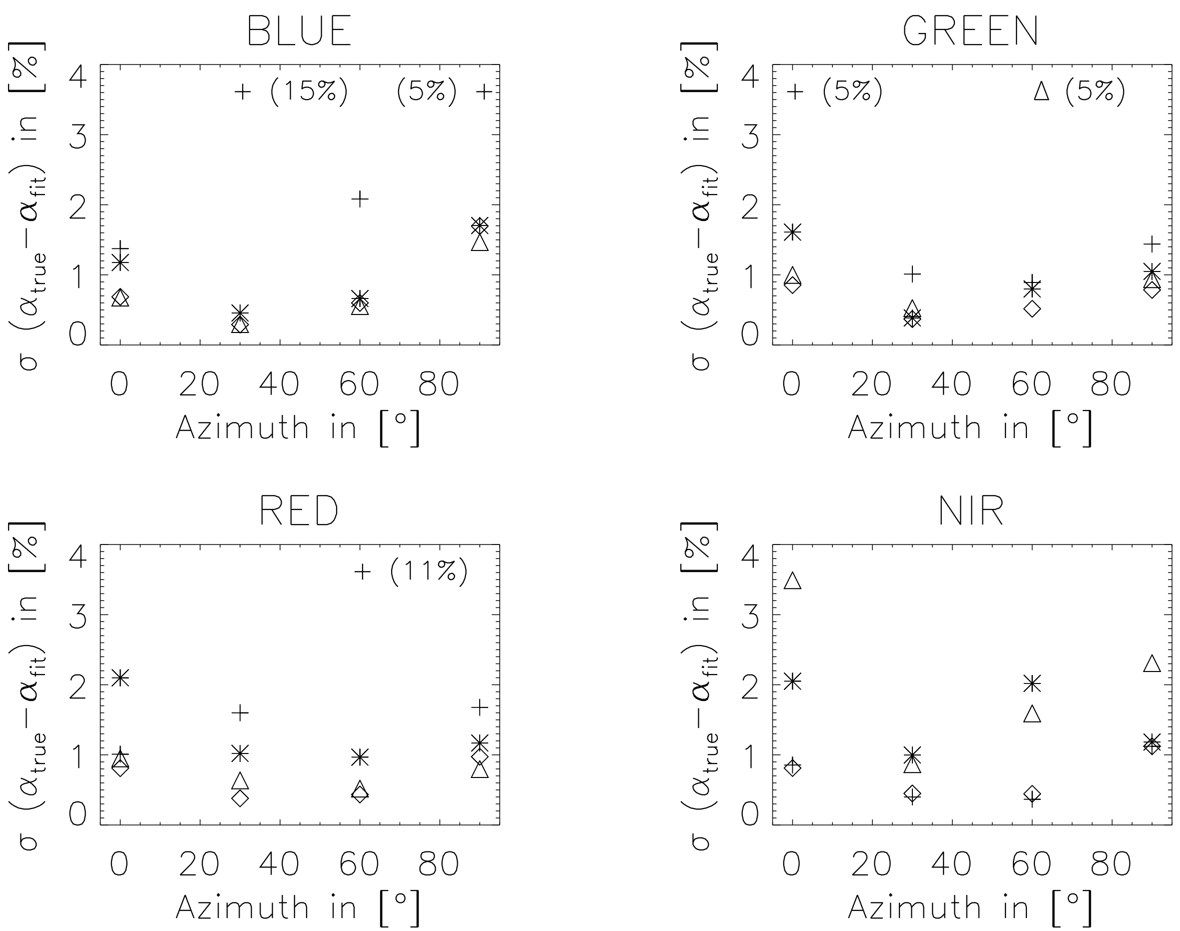

Symbols used: $\triangle$ Vegetation (23 models), $\diamond$ Soil and sand (3 models), $+$ Snow and ice (9 models) and $*$ Water (11 models).

Atmospheric Pre-Correction

Motivation: Visualizing the resulting TOA BRF fields for the BRF_1 and BRF_2 models we noticed that the BRF near the horizon ($80^o < \theta_v < 90^o$) often was very much larger than the computed BRF from JMRT.

Idea: Include atmospheric terms, e.g. transmission and path radiance from Rayleigh scattering.

$$\begin{aligned} BRF_4(\theta_i, \phi_i) &= BRF_{CSAR}(\theta_i, \phi_i; \varrho_0, \kappa, \Theta_0) \exp(-\tau_c/\mu_i) - BRF_{Rayleigh}(\theta_i, \phi_i) \\ &\quad , \; i = 1, 2, 3, \ldots, 9; \; c = 1, 2, 3, 4 \end{aligned} \tag{9}$$

and the albedo is given by the sum of:

$$\begin{aligned} \alpha_0 = Albedo(BRF_{CSAR,fit}(\theta_i, \phi_j) \exp(-\tau_c/\mu_i)) + Albedo(BRF_{Rayleigh}(\theta_i, \phi_j)), \\ i = 1, 2, 3, \ldots, N_\theta; \; j = 1, 2, 3, \ldots, N_\phi; \; c = 1, 2, 3, 4, \end{aligned} \tag{10}$$

where $BRF_{CSAR,fit}(\theta_i, \phi_j)$ is the hemispherical BRF computed from the best fit of the CSAR parameters to the BRF slice $BRF_4(\theta_i, \phi_i)$.

Result: Works well for blue channel and in the principle plane $\phi = 0^o$. Convergence problems, probably because no limits on the CSAR parameters is used.

Atmospheric Pre-Correction

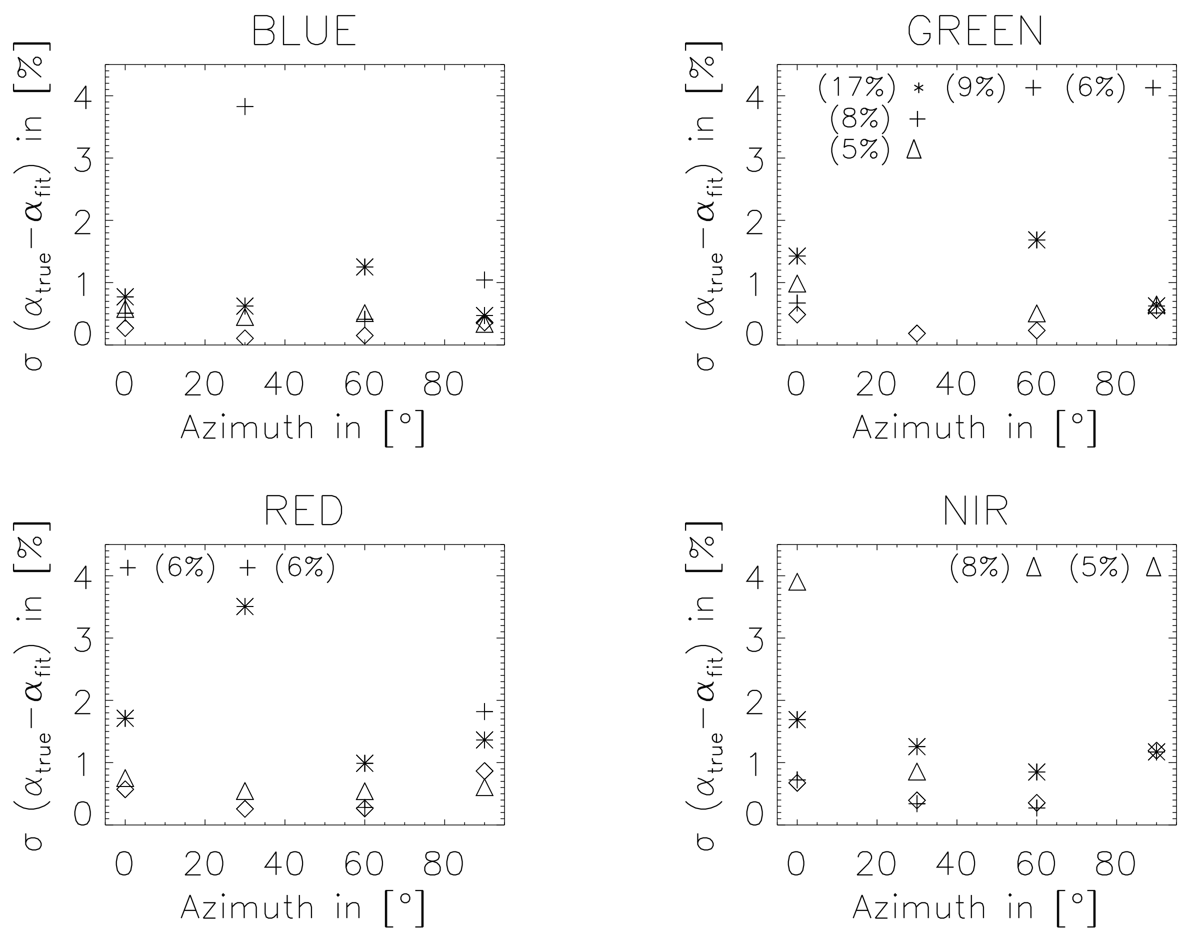

Symbols used: $\triangle$ Vegetation (23 models), $\diamond$ Soil and sand (3 models), $+$ Snow and ice (9 models) and $*$ Water (11 models).

Conclusions

- Albedo error is less than 1% in the visible and less than 1.5% in the NIR If only nadir measurements are used the albedo error is about 5 % in the visible and 10 % in the NIR.
- More work needed to make this approach robustly work for all surfaces and atmospheric conditions.
- Need to perform the inversion more rapidly and flag pixels for which the model did not fit very well.
- This approach lends itself to calculate the hemispherical BRF field over any region of the Earth.

Future Work

- Investigate other semi-empirical BRF models.
- How the BRF-CSAR parameters vary as a function of sun angle?
- Is there a diurnal smooth trajectory for a parameter with sun angle? If so, we could use this to predict the TOA clear sky albedo at times of the day.

Acknowledgments

This work was supported by the Multi-angle Imaging Spectro Radiometer (MISR) project through a contract from NASA/JPL. We recognize the significant contributions by Dr. Veronique Carrére (JRC, Ispra) and Heather Stephens (LANL) and Kerstin Lippert (LANL and DLR, Berlin).

References

Diner D.J., Clothiaux E., Conel J.E., Davies R., Di Girolamo L., Muller J.-P., Varnai T. and Wenkert D., 1994, MISR Level 2 Algorithm Theoretical Product: TOA/Cloud Product, JPL Report D-11399, March 3.

Nicodemus F.E., Richmond J.C., Hsia J.J., Ginsberg I.W. and Limperis T., 1977, Geometrical Considerations and Nomenclature for Reflectance, Washington, D.C.: NBS Monograph 160, National Bureau of Standards, Dept. of Commerce, p.52.

Rahman H., Verstraete M.M. and Pinty B., 1993, Coupled Surface-Atmosphere Reflectance (CSAR) Model (parts 1 and 2), JGR, 98:D11:20,779-20,789 and 98:D11:20,791-20,801.

Vermote E., Tanré D., Deuzé J.L., Herman M. and Morcette J.J., 1994, Second Simulation of the Satellite Signal in the Solar Spectrum, 6S User Guide Version n, NASA-Goddard Space Flight Center, Greenbelt, USA, p. 182.